Published in final edited form as:
Dev Biol. 2012 July 1; 367(1): 25–39. doi:10.1016/j.ydbio.2012.04.018.

The Engrailed Homeobox genes are required in multiple cell lineages to coordinate sequential formation of fissures and growth of the cerebellum

Grant D. Orvis[a], **Andrea L. Hartzell**[a], **Jenessa B. Smith**[a], **Luis Humberto Barraza**[a], **Sandra L. Wilson**[a], **Kamila U. Szulc**[b], **Daniel H. Turnbull**[b], and **Alexandra L. Joyner**[a,c]

[a]Developmental Biology Program, Sloan-Kettering Institute, 1275 York Avenue, New York, NY 10065, USA

[b]Structural Biology Program, Skirball Institute, New York University School of Medicine, 540 First Avenue, New York, NY 10016, USA

Abstract

The layered cortex of the cerebellum is folded along the anterior-posterior axis into lobules separated by fissures, allowing the large number of cells needed for advanced cerebellar functions to be packed into a small volume. During development, the cerebellum begins as a smooth ovoid structure with two progenitor zones, the ventricular zone and upper rhombic lip, which give rise to distinct cell types in the mature cerebellum. Initially, the cerebellar primordium is divided into five cardinal lobes, which are subsequently further subdivided by fissures. The cellular processes and genes that regulate the formation of a normal pattern of fissures are poorly understood. The engrailed genes (*En1* and *En2*) are expressed in all cerebellar cell types and are critical for regulating formation of specific fissures. However, the cerebellar cell types that *En1* and *En2* act in to control growth and/or patterning of fissures has not been determined. We conditionally eliminated *En2* or *En1* and *En2* either in both progenitor zones and their descendents or in the two complementary sets of cells derived from each progenitor zone. *En2* was found to be required only transiently in the progenitor zones and their immediate descendents to regulate formation of three fissures and for general growth of the cerebellum. In contrast, *En1* and *En2* have overlapping functions in the cells derived from each progenitor zone in regulating formation of additional fissures and for extensive cerebellar growth. Furthermore, *En1/2* function in ventricular zone-derived cells plays a more significant role in determining the timing of initiation and positioning of fissures, whereas in upper rhombic lip-derived cells the genes are more important in regulating cerebellar growth. Our studies reveal the complex manner in which the *En* genes control cerebellar growth and foliation in distinct cell types.

[c]Author for correspondence (joynera@mskcc.org).

Keywords

cerebellum; brain development; foliation; transcription factors; patterning; conditional knockouts; CRE

Introduction

Consisting of less than fifteen percent of the total volume in the brain, but containing more than fifty percent of its neurons, the murine cerebellum plays a key role in coordinating cell communication between the cerebral cortex and body (Llinas, 1975; Manto, 2008). In humans, the cerebellum controls precision and timing of locomotive movements, as well as higher order functions such as language acquisition, attention and emotional responses (Kandel et al., 2000; Manto, 2008). The cerebellum is patterned during development along the three axes. At the level of morphology the medial-lateral axis is subdivided into the vermis, paravermis, hemispheres and flocculi/paraflocculi, based on their distinct patterns of lobules (or folia) separated by fissures along the anterior-posterior axis (Altman and Bayer, 1997). The mammalian vermis can be divided into ten basic lobules (Larsell, 1952; Larsell, 1970) and in the murine vermis there are eight to ten lobules (I-X from anterior to posterior) depending on genetic strain, whereas only four lobules exist in the hemispheres. The production of lobules through the outgrowth of the surface of the cerebellum between fissures in higher organisms results in a great increase cell number, and thus the accommodation of more neural circuits compared to cerebella with a smoother surface. The pattern of the lobules is dependent upon the timing and placement of fissures, and it is therefore critical to study the genetic pathways that regulate formation of fissures in mammals. The generation of a complex structure such as the cerebellum requires precise regulation of cell specification, proliferation, differentiation and migration, and these processes must occur in a particular developmental sequence. Whereas genes required for specification and differentiation of various cell types in the cerebellum have been identified, genes that coordinate all the processes to produce the reproducible 3-dimensional structure of the cerebellum are poorly understood.

Development of the cerebellum begins with the specification of the cerebellar anlage from dorsal rhombomere 1 (r1), and in the mouse, this process begins at embryonic day 8.5 (e8.5) (Wingate and Hatten, 1999; Zervas et al., 2004). The cerebellum is unique in the brain in that it has two transcriptionally and spatially discrete progenitor zones: a ventricular zone (VZ) that lines the 4th ventricle, and a structure called the upper rhombic lip (RL) that runs along the posterior edge of the cerebellar anlage. The VZ expresses the pancreas transcription factor 1 alpha gene (*Ptf1a*) and gives rise to gamma-aminobutyric acid (GABAergic) interneurons, Purkinje cells and all glia, whereas the RL expresses *Atoh1* and produces all glutamatergic neurons including those of the deep cerebellar nuclei (DCN) and granule cells (gcs) of the internal granule cell layer (IGL) (Ben-Arie et al., 1997; Hashimoto and Mikoshiba, 2003; Hoshino et al., 2005; Machold and Fishell, 2005; Sudarov et al., 2011). Post-mitotic cells exiting the VZ primarily migrate radially and settle in specific layers of the cerebellar cortex, whereas cells exiting the RL initially migrate along the surface of the developing cerebellum (Altman and Bayer, 1997; Machold and Fishell, 2005).

DCN neurons leave the RL first and after reaching the rostral nuclear transitory zone descend ventrally and form three pairs of nuclei along the medial-lateral axis (Altman and Bayer, 1997). The granule cell precursors (gcps) in contrast form a proliferative secondary precursor zone on the surface of the cerebellum called the external granule cell layer (EGL) (Altman and Bayer, 1997). Post mitotic granule cells leave the EGL from e18.5 to postnatal day 16 (P16) and migrate down Bergmann glial fibers (a specialized glial cell) past the Purkinje cell layer to form the IGL. The granule cell axons (parallel fibers) form a progressive layer above the Purkinje cells called the molecular layer, which also houses two major interneuron subtypes (Altman and Bayer, 1997). How the correct number of each cell type is produced in each lobule has yet to be determined.

The process of creating lobules and sublobules through the progression of fissure formation, referred to as foliation, can be divided into two developmental stages (Altman and Bayer, 1997). The first stage of foliation begins at embryonic day 16.5 (e16.5) in the mouse and results in the production of five cardinal lobes in the vermis separated by four cardinal fissures, from anterior to posterior named the preculminate (pc), primary (pr), secondary (sec) and posterolateral (po) fissures (Altman and Bayer, 1997; Mares and Lodin, 1970) (see Fig. 7). None of the four cardinal fissures extend laterally through the entire hemispheres, although the primary fissure forms the anterior surface of the hemispheres. The second stage of foliation begins around birth and continues until the EGL is exhausted of cells (Altman and Bayer, 1997). This stage of development expands and divides the five cardinal lobes into lobules/sublobules as the Purkinje cells mature and spread from a multilayer into a monolayer (Altman and Bayer, 1997). The precentral fissure forms to separate a fused lobule I/II from III, and the prepyramidal fissure separates lobule VII from VIII. The first sign of formation of a fissure is an inward bulging of the inner surface of the EGL that is then followed by an indentation of the outer surface and accompanied by distinct changes in the organization of the surrounding cells, referred to as anchoring centers (Mares and Lodin, 1970; Sudarov and Joyner, 2007). However, the genetic mechanism(s) underlying the timing of initiation and positioning of fissures remains poorly understood.

The mouse engrailed1 (*En1*) and engrailed2 (*En2*) genes (Joyner et al., 1985; Joyner and Martin, 1987) encoding homeodomain transcriptional repressors are known to regulate many aspects of cerebellar patterning, including foliation (Cheng et al., 2010; Joyner et al., 1991; Millen et al., 1994; Sgaier et al., 2007) striped gene expression (Sillitoe et al., 2008) and afferent circuit topography (Sillitoe et al., 2010). In the mouse, *En1* expression begins at ~e8.0 and *En2* shortly thereafter in the mesencephalon (midbrain precursor) and r1 (Davis and Joyner, 1988; Davis et al., 1988). *En1/2* continue to be expressed throughout cerebellar development, but become spatially and temporally restricted to defined regions in the cerebellar anlage (Millen et al., 1995; Sgaier et al., 2007; Wilson et al., 2011). By e17.5, parasagittal groups of Purkinje cells express *En1/2* and granule cell precursors express *En1* primarily in the presumptive vermis and *En2* more broadly (Millen et al., 1995; Wilson et al., 2011). During postnatal development and in the adult, *En1* or *En2* continue to be expressed, but by P21 expression is restricted to subsets of Purkinje and DCN cells or granule cells, respectively, as well as interneurons (Wilson et al., 2011). While *En1/2* are known to have dynamic expression patterns throughout cerebellar development, the

relationship between the expression of these genes in particular cell types and their roles in regulating foliation remains to be elucidated.

Several studies of null and conditional *En1/2* mutants have defined overlapping and distinct requirements for *En1* and *En2* in cerebellar development. The earliest expression of *En1* is required for specification of the cerebellar anlage, as the absence of *En1* results in loss of the cerebellum by e9.5, unless the mutation is on a C57bl/6 background (Bilovocky et al., 2003; Wurst et al., 1994). In contrast, later expression of *En1* is not required for cerebellar foliation, as one third of outbred conditional mutants ($En1^{Cre/fx}$) that lack *En1* after e9, have normal cerebellar foliation (Sgaier et al., 2007). Unlike *En1*, *En2* is required after e12.5 for cerebellar foliation (Cheng et al., 2010; Joyner et al., 1991; Kuemerle et al., 1997; Millen et al., 1994). The vermal patterning defect in *En2* null mutants, a posterior shift of lobule VIII, results from a delay in formation of the secondary fissure and premature initiation of the prepyramidal fissure (Millen et al., 1994; Sudarov and Joyner, 2007). In the hemispheres, three rather than four lobules form due to lack of formation of the ansoparamedian fissure, resulting in the amalgamation of the CrusII and Paramedian lobules (Millen et al., 1994). Within their DNA binding domains, EN1 and EN2 share high homology and studies have demonstrated overlapping functions for the two proteins. For example, if the *En2* coding sequence is used to replace that of *En1* ($En1^{2ki/2ki}$ knock-in mice) the *En1* null phenotype is rescued (Hanks et al., 1995), whereas if *En1* in addition to *En2* is conditionally ablated after e14.5 ($R26^{CreER/+}$; $En1^{fx/-}$; $En2^{fx/-}$ mice given tamoxifen at e13.5 and e14.5) the size of the cerebellum is further reduced and additional lobules in the vermis are disrupted (Cheng et al., 2010; Sgaier et al., 2007). The *En2* null mutant hemisphere foliation phenotype is only reproduced, however, if *En2* (or both *En* genes) are inactivated by e11. While these studies revealed a role for *En1/2* in regulating foliation and growth after e14.5, the cells in which the *En* genes function to regulate cerebellar development were not defined.

As a means to understand how the *En* genes regulate foliation and growth of the cerebellum, we inactivated *En2* alone or *En1* and *En2* in cells of the two progenitor zones and/or their descendents. Inactivation of *En1/2* in both progenitor zones at ~e10.5 resulted in a profound inhibition of expansion of the vermis. In contrast, deletion of the *En* genes in the cells derived from the two progenitor zones revealed that both *En1* and *En2* are required within these cells for foliation and general growth. Moreover, combined EN1/2 function is required independently in VZ- and RL-derived cells to regulate foliation, with VZ-derived cells playing a greater role. In addition, RL-derived cells play a prominent role in cerebellar growth. Finally, developmental studies uncovered distinct alterations in the timing of formation of particular fissures depending on the cell types in which the *En* genes are intact. Thus, *En1* and *En2* act together in multiple cerebellar cell types to determine overall growth and formation of particular fissures. In this way the *En* genes are critical for determining the number of cells allocated to each lobule and thus the cells available to participate in particular neural circuits.

MATERIALS AND METHODS

Mice

All mouse lines have been previously described and were maintained on a mixed, predominantly Swiss Webster genetic background: *Nestin-Cre (*Tronche et al., 1999), *Ptf1a*^{Cre} (Kawaguchi et al., 2002), *Atoh1-Cre (*Matei et al., 2005), *Rosa26*^{lacZ}(Soriano, 1999), *En1*^{lacZ} (Hanks et al., 1995), *En1*^{fx} (Sgaier et al., 2007), *En2*^{hd} (Joyner et al., 1991), *En2*^{fxlacZ} (Cheng et al., 2010; Sgaier et al., 2005) and *En2*^{fx} (Cheng et al., 2010).

Tissue preparation and histology

Adult cerebella were collected at P28-P32 following cardiovascular perfusion and then fixed overnight in 4% paraformaldehyde (PFA) at 4°C, whereas embryonic and early postnatal cerebella were collected and fixed overnight without cardiovascular perfusion. Tissue was dehydrated through an ethanol series and embedded in paraffin for histological sectioning at 7μm, and counter stained with hematoxylin and eosin. Tissue collected for immunofluorescence and X-gal staining of *Cre; R26*$^{lacZ/+}$ animals was dehydrated in 30% sucrose and frozen. Frozen tissue was sectioned at 12μm or 16μm for immunofluorescence and at 14μm for e15.5 embryos and 40μm for P30 adults for X-gal stained tissue.

Immunofluorescence

Sectioned tissue was washed first with PBS and then with 0.25% Triton-X 100 in phosphate buffered saline (PBT). The samples were blocked with 5% bovine serum albumin (BSA) in 0.5% PBT at room temperature for one hour. Antibodies used were: affinity purified rabbit anti-Enhb1 (Davis et al., 1991), mouse anti-Calbindin1 (Swant 300), rabbit anti-Pax6 (Millipore AB2237). The antibodies were diluted in 5% BSA/PBT at dilutions of 1:100, 1:1000 and 1:500, respectively and incubated overnight at 4°C. Following primary antibody incubation, the slides were washed at room temperature with PBS. An Alexa Fluor donkey anti-rabbit or anti-mouse FITC conjugated IgG secondary antibody was diluted in 0.5% PBT at 1:500 and applied to the samples at room temperature for one hour. The slides were washed with PBS and then mounted with Fluorogel containing Tris Buffer.

Magnetic resonance microimaging and volumetric analysis

Adult mice were collected through cardiovascular perfusion with a 10mM solution of gadopenetate dimeglumine (Magnevist, Bayer HealthCare Pharmaceuticals) in 0.9% PBS mixed with heparin (5000 u/L). The initial flush was followed by 4% paraformaldehyde (PFA) at 4°C mixed with 10mM Magnevist. The brains were left in the skulls, kept at 4°C in 3.5mM solution of contrast agent in 4% PFA until imaging 48–76h after perfusion. Heads were imaged 4 at a time. For imaging the samples were transferred to a custom holder and immersed in perfluoropolyether (Fomblin, Solvay Solexis) for the duration of the scan. The MRI data was collected on a 7T micro-MRI (Bruker Biospec) using 750mT/m actively shielded gradients (BGA 09S, Bruker) and a 32-mm (ID) volume coil (Doty Scientific). The sequence parameters were: TE/TR=6.26/50ms, FA=40°, FOV=3.0cm^3, matrix=512^3, NEX=2, resolution=59μm isotropic and imaging time of 7h 17 min. Volumetric analysis of the whole brain, the whole cerebellum and cerebellar sub regions were performed using

AMIRA (Visage Imaging) using the semi-automated segmentation option that was corrected manually. Volumes of structures of interest were calculated by multiplying the number of voxels in the ROI by the volume of an individual voxel.

RESULTS

Strategy to generate *En1* and *En2* progenitor zone-specific cerebellar conditional mutants

To test whether expression of *En2* alone or *En1* and *En2* in the distinct cell types produced by each progenitor zone regulates different aspects of cerebellar development, we utilized three different *Cre* expressing alleles to eliminate *En1/2* function. To conditionally inactivate *En1/2* in the VZ and RL, we used a *Nestin-Cre* transgene (Tronche et al., 1999) which induces recombination throughout the cerebellar anlage at ~e10.5 (Blaess et al., 2006). Therefore, use of the *Nestin-Cre* transgene allows for deletion of *En1/2* in the VZ and RL (neural progenitors), as well as their progeny and is referred to as *NP-Cre*. We utilized a $Ptf1a^{Cre}$ knock-in allele (Kawaguchi et al., 2002) and an *Atoh1-Cre* transgene (Schuller et al., 2007) to conditionally inactivate *En1/2* in VZ-derived or RL-derived cells, respectively. The $R26^{lacZ}$ conditional reporter allele (Soriano, 1999) was used to assess *Cre* activity based on beta-galactosidase (β-gal) enzyme activity in mice carrying each *Cre* allele. Recombination with the $Ptf1a^{Cre}$ allele was seen in a majority of cells in the cerebellar cortex at e15.5 (Suppl. Fig. 1E & F). Importantly, at e15.5 few β-gal positive cells were detected in the ventricular zone or EGL (Suppl. Fig. 1E & F). In adult $Ptf1a^{Cre/+}$; $R26^{lacZ/+}$ mice, β-gal activity was detected in most GABAergic neurons (as identified by cell position and shape) including Purkinje cells and interneurons, in addition to a small percentage of cells in the IGL in a decreasing gradient from anterior to posterior (Suppl. Fig. 1G & H) (Hoshino et al., 2005). Therefore, the $Ptf1a^{Cre/+}$ allele recombines in cells derived from the ventricular zone and is referred to as *VZd-Cre*. At e15.5, recombination with the *Atoh1-Cre* allele had occurred in cells of the anterior EGL and nuclear transitory zone, as well as a few cells within the cerebellar cortex, but not the posterior EGL or RL (Suppl. Fig. 1I & J). In adult *Atoh1-Cre/+;* $R26^{lacZ/+}$ mice, β-gal activity was detected in the DCN and in nearly all cells in the IGL of lobules I-VIII, with a decreasing gradient of β-gal activity posterior to the secondary fissure (lobules IX-X) (Suppl. Fig. 1K & L). Therefore, the *Atoh1-Cre/+* allele recombines in cells derived from the rhombic lip and is referred to as *RLd-Cre*. As expected, in e15.5 embryos and adult mice carrying both *Cre* drivers (*RLd-Cre; VZd-Cre;* $R26R^{lacZ/+}$) β-gal activity was detected in most cells throughout the medial-lateral axis of the cerebellar primordium with the exception of the ventricular zone, posterior EGL and RL (Suppl. Fig. 1A–D). Therefore, utilization of the *VZd-Cre* and *RLd-Cre* alleles allows for conditional inactivation of *En1/2* primarily in VZ-derived and RL-derived cells, respectively, soon after they leave each progenitor zone.

Two sets of *En1/2* conditional mutants were generated, the first carried both a null and floxed (*fx*) allele for *En2* alone ($En2^{fx/-}$) or for each *En* gene ($En1^{fx/-}$; $En2^{fx/-}$) and the second set were homozygous for the floxed alleles ($En1^{fx/fx}$; $En2^{fx/fx}$). The generation of mutant animals with null alleles allowed for the analysis of an allelic series of *En1/2* conditional mutants (*Cre* allele plus $En1^{fx/+}$; $En2^{fx/-}$ or $En1^{fx/-}$; $En2^{fx/+}$ versus $En1^{fx/-}$; $En2^{fx/-}$) and therefore insight into which *En* gene is required to a greater degree for a

particular process of cerebellar development. Since ~10% of *En1*$^{+/-}$; *En2*$^{+/-}$ animals exhibit a mild patterning defect in the vermis (Sgaier et al., 2007), this must be taken into account when making conclusions about the various phenotypes using mice heterozygous for *En* null alleles. The numbers of *En2* alone or *En1/2* double mutants analyzed for each genotype and their relative phenotypes is summarized in Table 1. Investigation of *En1/2* function employing the *En1*$^{fx/fx}$; *En2*$^{fx/fx}$ alleles and a breeding scheme involving crossing *Cre*$^{+/-}$; *En1*$^{fx/fx}$; *En2*$^{fx/fx}$ and *En1*$^{fx/fx}$; *En2*$^{fx/fx}$ mice is the most efficient way to generate mutant and control littermates, and thus these alleles were used to analyze *En1/2* function at multiple developmental stages. The phenotypes of conditional *En1/2* mutants were similar regardless of which of the two sets of alleles were used (Table 1). Furthermore, in figures with phenotypes, stars denote fissures with developmental defects and yellow highlighted areas denote regions with defects in mutants compared to same region in the control.

En2 is required in cells of the two progenitor zones and only their immediate descendents for normal cerebellar foliation and growth

As a first step towards determining in what cell subtypes the *En* genes are required for cerebellar patterning, we eliminated *En2* function within the VZ and RL or within only the progeny of the two zones and analyzed cerebellar morphology. As expected, loss of *En2* from the two progenitor zones (*NP-Cre; En2*$^{fx/-}$) resulted in a phenotype identical to that of *En2*$^{-/-}$ mutants: an overall decrease in the size of the cerebellum, a specific posterior shift of lobule VIII in the vermis, and a fusion of the CrusII and Paramedian lobules in the hemispheres (Fig. 1A–F and Table 1) (n=4). These phenotypes have been shown to result from changes in the timing of formation of the fissures in the vermis surrounding lobule VIII such that there is a delay in initiation of the secondary fissure and a premature formation of the prepyramidal fissure and in the hemispheres, the ansoparamedian fissure that normally forms between the CrusII and Paramedian lobules does not form. In contrast to *NP-Cre; En2*$^{fx/-}$ mutants, loss of *En2* from both the VZ- and RL-derived cells (*RLd-Cre; VZd-Cre; En2*$^{fx/-}$) did not result in a foliation or size defect (Fig. 1G & H and Table 1) (n=4). Likewise, removal of *En2* from only VZ-derived (*VZd-Cre; En2*$^{fx/-}$) (n=2) or RL-derived cells (*RLd-Cre; En2*$^{fx/-}$) (n=3) did not result in any phenotype (Fig. 1I–L and Table 1). Surprisingly, these results suggest that *En2* is dispensable outside of the VZ and RL for regulating cerebellar foliation and growth. Two possible explanations for this finding are that *En1* can compensate for loss of *En2* outside the VZ and RL, or that EN2 protein persists in VZ- and RL-derived cells and this preserves the normal development.

As one approach to distinguish between these possibilities we utilized an allele to conditionally restore *En2* function in an otherwise *En2*$^{-/-}$ mutant background, which we define as ‘conditional restoration’ of a silenced allele (Cheng et al., 2010; Sgaier et al., 2005). The reasoning being that EN2 expression will be restored faster with conditional restoration than EN2 protein is degraded after gene ablation. Animals homozygous for the conditional restoration allele (*En2*$^{fxlacZ/fxlacZ}$) display an *En2*$^{-/-}$ patterning phenotype (Fig. 2A–D) (n=4) (Cheng et al., 2010). As expected, conditional restoration of *En2* in the VZ and RL (*NP-Cre; En2*$^{fxlacZ/fxlacZ}$) resulted in a complete rescue of the *En2*$^{-/-}$ foliation and size defects (Fig. 2E & F and Table 1) (n=4). Interestingly, conditional restoration in both the VZ- and RL-derived cells (*RLd-Cre; VZd-Cre; En2*$^{fxlacZ/fxlacZ}$) also rescued the mutant

phenotypes in the vermis and hemispheres (Fig. 2G & H and Table 1) (n=3). However, conditional restoration of *En2* in only VZ-derived cells (*VZd-Cre; En2*$^{fxlacZ/fxlacZ}$) did not rescue the foliation or size defects (Fig. 2I & J and Table 1) (n=4), whereas conditional restoration in RL-derived cells (*RLd-Cre; En2*$^{fxlacZ/fxlacZ}$) resulted in a partial rescue only of the *En2*$^{-/-}$ vermis foliation defect. In 3 out of 5 *RLd-Cre; En2*$^{fxlacZ/fxlacZ}$ mutants only a partial posterior shift of lobule VIII was detected, but the CrusII and Paramedian lobules were fused and the cerebellum reduced in size in all mutants (Fig. 2K & L and Table 1). The rescue of the *En2* null phenotype in *En2*$^{fxlacZ/fxlacZ}$ mice using *RLd-Cre* and *VZd-Cre* compared to no mutant phenotype produced when the two *Cre* alleles are used to remove *En2* function is likely explained by an earlier timing in the activation of *En2* function using the restoration allele than the timing of degradation of EN2 protein after the floxed allele is deleted using the same *Cre* drivers. Indeed, analysis of the *Cre* drivers with *R26*$^{lacZ/+}$ revealed β-gal activity (and thus EN2 function) begins as early as e11.5 and e12.5 with the *RLd-Cre* and *VZd-Cre* alleles, respectively (Suppl. Fig. 2A & B), whereas loss of EN1/2 protein in double conditional mutants is significantly delayed (see below). Taken together, these results demonstrate an early requirement for *En2* in cells of the VZ and RL and likely also in the cells immediately derived from both progenitor zones for normal cerebellar foliation and growth.

Expansion of the vermis requires continuous *En1/2* expression

Since a *R26*^{CreER} allele was employed in a previous study that showed *En1/2* are required after e15.5 for foliation and growth, recombination with CREER was not complete and some cells of the cerebellum continued to express *En1/2* (Cheng et al., 2010). As a means to avoid this problem and to delay deletion of *En1/2* in the VZ and RL until after the cerebellar anlage is specified (~e10.5), we utilized *NP-Cre* to ablate *En1/2*. Unlike using the *R26*^{CreER} allele with injection of tamoxifen at e10.5, inactivation of *En1/2* within the VZ and RL after e10.5 (*NP-Cre; En1*$^{fx/-}$; *En2*$^{fx/-}$) led to early postnatal death, as mutants failed to feed and also exhibited breathing difficulties similar to *En1* null mutants (Wurst et al., 1994). We therefore analyzed mutants at birth when the four cardinal fissures have formed in the vermis of normal mice (Fig. 3A & B). Strikingly, loss of *En1/2* using *NP-Cre* resulted in a cerebellum without fissures at P0, as well as a severe hypoplasia of the vermis (n=3) (Fig. 3C & D). To determine if the medial cerebellum was specified prior to *En1/2* loss, we analyzed calbindin (CALB1) and PAX6 expression, markers of Purkinje and granule cells, respectively. In *NP-Cre; En1*$^{fx/-}$; *En2*$^{fx/-}$ mutants, both cell type markers were detected at the midline, indicating that the cerebellar anlage had been specified (Suppl. Fig. 3A, B, D & E). Furthermore, we performed analysis of EN1/2 protein in these mutants and observed no expression of EN1/2 in mutants at birth (Suppl. Fig. 3C & F). Our results demonstrate that *En1/2* are required after e10.5 for normal expansion of the cells in the presumptive vermis.

Loss of three alleles of *En1* or *En2* such that one functional allele of *En1* or *En2* remained, (*NP-Cre; En1*$^{fx/+}$; *En2*$^{fx/-}$ or *NP-Cre; En1*$^{fx/-}$; *En2*$^{fx/+}$, respectively) resulted in a less severe hypoplasia of the vermis than in mutants lacking both *En1* and *En2* (Fig. 3E–H). Furthermore, both conditional mutants carrying one wild-type *En* allele survived to adulthood. We therefore analyzed the adult cerebellar phenotypes and compared them to *En1*$^{+/-}$; *En2*$^{-/-}$ mutants (Sgaier et al., 2007). Interestingly, conditional mutants with one

functional allele of *En1* after ~e10.5 (*NP-Cre; En1*$^{fx/+}$*; En2*$^{fx/-}$) had foliation patterning defects comparable to those of *En1*$^{+/-}$; *En2*$^{-/-}$ mutants (Fig. 3I–N) (n=3). In the midline (vermis), the relative depth of the prepyramidal fissure was greater than normal and a distinct secondary fissure was not present, but a small bulge in the IGL on the anterior face of lobule IX likely demarcated what remained of lobule VIII (Fig. 3M). In the anterior cerebellum, the primary fissure appeared to be missing in all mutants (3/3) and the precentral fissure was shortened (2/3) (Fig. 3M and Table 1) (see alternative interpretation below). In the hemispheres, although four lobules were present, the CrusII and Paramedian lobules were fused due to a missing ansoparamedian fissure (as in *En2* null mutants) and an ectopic anterior lobule was present (see below) (Fig. 3N and Table 1). Interestingly, adult conditional mutants with one functional allele of *En2* (*NP-Cre; En1*$^{fx/-}$; *En2*$^{fx/+}$) exhibited a less severe phenotype in the vermis with only a shortened secondary and relatively deeper prepyramidal fissures in the posterior as well as a missing (3/4) or shortened (1/4) precentral fissure in the anterior cerebellum (Fig. 3I, K & O and Table 1). In the hemispheres the ansoparamedian fissure formed in a manner comparable to control animals (n=4) (Fig. 3J, L & P and Table 1). Thus, as found previously using an *En1* knock-in allele expressing *En2* and removing the endogenous *En2* gene (*En1*$^{En2/En2}$; *En2*$^{-/-}$; Sgaier et al, 2007), *En2* supports patterning of foliation to a greater extent than *En1* (Table 1).

Our analyses of an allelic series of *NP-Cre* conditional mutants, along with previous studies demonstrate a role for *En1* and *En2* acting together to promote formation of fissures within anterior lobules, as well as the prepyramidal and secondary fissures that define lobule VIII (Fig. 3) (Cheng et al., 2010; Sgaier et al., 2007; Sillitoe et al., 2008). In most wild-type animals at the midline, the anterior cerebellum (lobules I-V) contains three fissures from anterior to posterior: the precentral fissure, preculminate fissure and primary fissure. The preculminate and primary cardinal fissures are easily identified as the two deepest fissures in the mature cerebellum with the more shallow precentral fissure forming after birth (Altman and Bayer, 1997). Between the primary and preculminate fissures, a lobule consisting of a fusion of lobules IV and V (seen in some mammals) normally forms (Fig. 3I). Previous studies of *En1/2* conditional knockouts or *En1*$^{+/-}$*; En2*$^{-/-}$ mutants indicated the anterior foliation defect to result from a fusion of lobules I-V suggesting that the preculminate fissure fails to form in these mutants (Cheng et al., 2010; Sgaier et al., 2007; Sillitoe et al., 2008). In order to determine the identity of the anterior fissures in *En1/2* progenitor zone conditional mutants, the continuity of fissures along the medial to lateral axis was ascertained. In control animals, when the primary and preculminate fissures are followed from the midline laterally, only the primary fissure extends into the hemispheres and eventually becomes the anterior face of the most anterior lobule (Simplex), whereas the preculminate fissure disappears within the paravermis (Fig. 4A–E). In the vermis of *NP-Cre; En1*$^{fx/+}$; *En2*$^{fx/-}$ mutants however, only one deep anterior fissure was present and it extended laterally to become the anterior face of the most anterior lobule in the hemispheres (Fig. 4F–J). Curiously however, in all animals analyzed (n=3), an additional fissure formed lateral to the midline that was posterior to the deep anterior vermal fissure and it extended laterally into the hemispheres, creating an ectopic anterior lobule in the hemispheres (Fig. 4H–J). One interpretation of the foliation pattern is that a shallow precentral fissure and a deep preculminate fissure forms at the midline. Additionally, the preculminate fissure

extends abnormally into the hemispheres and becomes the anterior face of the hemispheres. Furthermore, the primary fissure fails to form at the midline, but does form laterally and extends into the hemispheres. In this scenario, an ectopic lobule forms in the anterior portion of the hemispheres between the laterally extended primary fissure and the abnormally extended preculminate fissure (see labeling in Fig. 4F–J). An alternative interpretation is that the primary fissure and either the precentral or preculminate fissure form at the midline, but not the preculminate or precental fissure, respectively, and as in normal mice the primary fissure extends lateral becoming the anterior face of the hemispheres. In this second scenario, an ectopic fissure would develop posterior to the primary fissure in the paravermis that extends into the hemispheres. An extra lobule therefore would be created in the hemispheres between the ectopic fissure and the anterior face of the hemispheres (primary fissure).

In contrast to *En1/2* conditional mutants expressing only one allele of *En1*, in *NP-Cre; En1*$^{fx/-}$; *En2*$^{fx/+}$ mutants expressing one allele of *En2*, two deep anterior fissures were present at the midline. The fissures likely represent the primary and preculminate fissures as they extended laterally in a manner similar to control cerebella. The precentral fissure therefore was greatly reduced or did not form in the mutants (Fig. 4K–O and Table 1). These results along with data presented below provide strong evidence that in the anterior cerebellum, *En1/2* primarily regulate development of the primary and precentral fissures.

En1/2 are independently required in ventricular zone-derived and upper rhombic lip-derived cells to enhance cerebellar growth and for fissure formation in the vermis

In order to test whether cerebellar growth and formation of fissures requires *En1/2* in VZ- and/or RL-derived cells we utilized the *VZd-Cre* and *RLd-Cre* alleles. In contrast to *NP-Cre; En1*$^{fx/+}$; *En2*$^{fx/-}$ conditional mutants, conditional loss of *En1* and *En2* in both VZ- and RL-derived cells (*RLd-Cre; VZd-Cre; En1*$^{fx/-}$; *En2*$^{fx/-}$) did not result in lethality (n=5). However, unlike *RLd-Cre; VZd-Cre; En2*$^{fx/-}$ mice which have normal cerebellar morphology, in the posterior vermis of *RLd-Cre; VZd-Cre; En1*$^{fx/-}$; *En2*$^{fx/-}$ mutants lobule VIII and the secondary fissure were absent (Fig. 5A & C and Table 1). Furthermore, anterior patterning defects were also observed and the overall size of the vermis and hemispheres was greatly reduced in all mutants. Interestingly, the ansoparamedian fissure in the hemispheres formed normally in *RLd-Cre; VZd-Cre; En1*$^{fx/-}$; *En2*$^{fx/-}$ mutants (Fig. 5B & B and Table 1). Analysis of anterior fissures along the medial-lateral axis revealed the presence of the preculminate fissure (5/5) a missing (2/5) or shortened (3/5) primary fissure and a missing (2/5) or shortened precentral (3/5) fissure at the midline (Fig. 5A & C, Table 1 and Suppl. Fig. 4F–J). In the mutants without a primary fissure at the midline a primary fissure was present laterally and extended into the hemisphere to become the anterior face of the Simplex lobule (5/5) (Suppl. Fig. 4F–J). Taken together with our analysis of *RLd-Cre; VZd-Cre; En2*$^{fx/-}$ mutants which have normal cerebellar morphology, our analysis of *RLd-Cre; VZd-Cre; En1*$^{fx/-}$; *En2*$^{fx/-}$ mutants reveals that *En1* and *En2* act together in VZ- and RL-derived cells to promote vermal foliation and overall cerebellar growth.

Interestingly, inactivation of *En1/2* from only VZ-derived cells (*VZd-Cre; En1*$^{fx/-}$; *En2*$^{fx/-}$) resulted in a missing or (2/5) shortened (3/5) secondary fissure with a deeper than normal

prepyramidal fissure (5/5), as well as a shortened primary fissure (3/5) and precentral fissure (1/5) (Fig. 5A & E and Table 1). In contrast, conditional inactivation of *En1/2* in RL-derived cells (*RLd-Cre; En1*$^{fx/-}$; *En2*$^{fx/-}$) resulted in an obvious hypoplasia in all mutants (n=4), a shortened secondary fissure (2/4), a shortened primary fissure (2/4) and a missing precentral fissure (2/4) (Fig. 5A & G and Table 1). We next determined the volume of the cerebellum in *RLd-Cre; En1*$^{fx/fx}$; *En2*$^{fx/fx}$ conditional mutants using anatomical MRI (n=6). Total cerebellar volume was decreased by 20% (p=0.004) (Fig. 5I), whereas the volume of the vermis was decreased by 25% (p=0.001) (Fig. 5J) and the hemispheres displayed an 18% (p=0.019) decrease in overall volume (Fig. 5K). Thus, expression of *En1/2* in either VZ- or RL-derived cells partially rescues the anterior and posterior patterning defects seen when *En1/2* are deleted in both cell populations. Furthermore, *En1/2* expression in VZ-derived cells seems to be more critical for patterning fissures, whereas *En1/2* expression in RL-derived cells is more critical for overall cerebellar growth.

To determine which *En* gene is most required in VZ- and RL-derived cells, we analyzed additional conditional mutants containing one intact allele of *En1* or *En2* with one or two *Cre* drivers. Curiously, in all *RLd-Cre; VZd-Cre; En1*$^{fx/+}$; *En2*$^{fx/-}$ or *RLd-Cre; VZd-Cre; En1*$^{fx/-}$; *En2*$^{fx/+}$mutants (n=4 or n=3), a similar phenotype was observed: lobule VIII was shifted posterior as in *En2* null mutants (Fig. 6E–H and Table 1). When only one allele of *En1* was present in VZ-derived cells (*VZd-Cre; En1*$^{fx/+}$; *En2*$^{fx/-}$ mutants) a mild posterior shift of lobule VIII was seen in all mutants (n=3). In contrast, when one allele of *En2* was present in VZ-derived cells (*VZd-Cre; En1*$^{fx/-}$; *En2*$^{fx/+}$) (n=5), no foliation defects were observed (Fig. 6I–L and Table 1). When one allele of *En1* was present in RL-derived cells (*RLd-Cre; En1*$^{fx/+}$; *En2*$^{fx/-}$) lobule VIII was shifted posterior in only one mutant (Fig. 6M & N and Table 1) (n=3), and again when one allele of *En2* was present in RL-derived cells (*RLd-Cre; En1*$^{fx/-}$; *En2*$^{fx/+}$) no foliation defects were detected (Fig. 6O & P and Table 1) (n=5). These results demonstrate that one functional allele of *En1* or *En2* expressed in both VZ- and RL-derived cells is sufficient to rescue the anterior but not the posterior foliation defects seen when all four *En* alleles are removed from the cells. In addition, the growth defect is largely rescued. Furthermore, in either VZ-derived or RL-derived cells alone, *En2* function, but not *En1* is sufficient to restore normal foliation to the double mutants.

En1 and *En2* are differentially required in ventricular zone- and upper rhombic lip-derived cells for timing of initiation of particular vermal fissures

To further address which fissures are disrupted when *En1* and *En2* are removed from the cells derived from one or both progenitor zones, and to determine whether the sequence of fissure formation is altered as in *En2* mutants, we analyzed the continuity of fissures along the medial-lateral axis of the cerebellum at three postnatal stages when fissures are forming in the *En1/2* conditional mutants (P1, P3 & P5) (Fig. 7 and Suppl. Fig. 6). To aid in our analysis, we generated outlines of midline sections of each animal and superimposed them on outlines of littermate controls (Fig. 8). In all conditional mutants generated, a delay in the initiation of all fissures was observed and the fissures that formed most normally in all mutants were the preculminate and posterolateral cardinal fissures (Fig. 7). As expected, conditional inactivation of *En1/2* in both VZ- and RL-derived cells (*RLd-Cre; VZd-Cre; En1*$^{fx/fx}$; *En2*$^{fx/fx}$) resulted in the most severe developmental phenotype with no fissures

formed by P1 at the midline (Fig. 7A & E and Fig. 8A & D) (n=2). At P3, four fissures were present: two deeper fissures, the preculminate and posterolateral, and two shallower fissures between them, the primary and prepyramidal (Fig. 7B & F and Fig. 8B & E) (n=3). At P5, a shallow primary fissure was detected in 2 of 3 mutants but the secondary fissure was still absent in all mutants, the prepyramidal fissure was as deep as in the larger control cerebella (3/3) and the precentral fissure had a relatively normal depth (3/3) (Fig. 7C & G and Fig. 8C & F). In mutants where the primary fissure was not present at the midline, it was present laterally in the paravermis and formed the anterior face of the Simplex lobule of the hemispheres (Suppl. Fig. 6F–J). These results are consistent with the phenotypes seen in adult conditional mutants: a shortened or missing primary fissure, and an absence of lobule VIII due to alterations in formation of the secondary and prepyramidal fissures.

Conditional inactivation of *En1/2* in the VZ-derived cells (*VZd-Cre; En1*$^{fx/fx}$; *En2*$^{fx/fx}$) resulted in a less severe patterning phenotype in the adult compared to *RLd-Cre; VZd-Cre; En1*$^{fx/fx}$; *En2*$^{fx/fx}$ mutants and similarly, a less severe phenotype was observed during development (Fig. 7I–K and Fig. 8G–I). In anterior lobules at P1, both the preculminate and primary fissures formed, but not the precentral fissure. However, outgrowth of the lobules was delayed in comparison to littermate control animals (3/3) and patterning of the posterior lobules was altered with the premature formation of the prepyramidal fissure and a shortened (1/3) or missing secondary fissure (2/3) (Fig. 7A & I and Fig. 8A & G). By P3, the primary fissure was shorter rather than longer than the preculminate fissure (3/3), the precentral fissure was present (3/3), the prepyramidal fissure was relatively deeper than normal (3/3) and the secondary fissure was shortened (1/3) or missing (2/3) (Fig. 7B & J and Fig. 8B & H). Comparably, at P5 in the midline a shallow primary fissure (4/4), a shortened precentral (1/4), a relatively deeper prepyramidal (4/4) and shallow (1/4) or missing (3/4) secondary fissure were observed (Fig. 7C & K and Fig. 8C & I).

Similar to the adult, conditional inactivation of *En1/2* in RL-derived cells (*RLd-Cre; En1*$^{fx/fx}$; *En2*$^{fx/fx}$) resulted in an obvious decrease in the size of the cerebellum, as well as mild foliation patterning defects in the anterior and posterior cerebellum during development (Fig. 7M–O and Fig. 8J–L). In all *RLd-Cre; En1*$^{fx/fx}$; *En2*$^{fx/fx}$ mutants at all stages, loss of *En1/2* resulted in a greatly shortened primary fissure at the midline (Fig. 7A–C & M–O and Fig. 8A–C & J–L). In addition, the precentral fissure was not present at P1 (4/4) or at P3 (2/4) and at P5 was shortened (1/4) or missing (1/4) (Fig. 7A–C & M–O and Fig. 8A–C & J–L). In the posterior cerebellum, the secondary fissure was present, but not the prepyramidal fissure in all mutants at all stages (Fig. 7A– C & M– O and Fig. 8A–C & J–L). Since in adult mutants, both the prepyramidal and secondary fissures are present at the midline (Fig. 5G and Suppl. Fig. 5G), the prepyramidal fissure must form at the midline after P5. Consistent with this, analysis of fissures along the medial-lateral axis revealed that at P5 the prepyramidal fissure was present in the paravermis (Suppl. Fig. 6P–T). Analysis of e18.5 mutants revealed that formation of the secondary fissure was delayed (data not shown and see Fig. 10). These results demonstrate a major delay in formation of the prepyramidal fissure when *En1/2* expression is eliminated from RL-derived cells. Taken together, our analysis of foliation in a series of *En1/2* conditional mutants has revealed that expression of *En1/2* is essential independently in the VZ- and RL-derived cells for normal timing of

initiation of the precentral, primary, prepyramidal and secondary fissures. Moreover, *En1/2* function positively or negatively on formation of the prepyramidal fissure depending on whether they are functioning in RL or VZ-derived cells, respectively, and most prominently in VZ-derived cells to promote formation of the secondary fissure. In addition, as in *En2* mutants (Millen et al., 1994; Sudarov and Joyner, 2007) the characteristic changes in cellular cytoarchitecture seen at the base (anchoring center) of each fissure appeared to be normal in all the conditional mutants once a fissure began to form (e.g. see Fig. 7 and 10).

The significant decrease in cerebellar size of *RLd-Cre; En1$^{fx/fx}$; En2$^{fx/fx}$* raises the question of whether the size decrease is a result of only a decrease in granule cells or whether other cell types are also reduced. Previous experiments have demonstrated that the cerebellum can be decreased in size due to loss of granule cells without a corresponding decrease in Purkinje cell number, and in such mutants the Purkinje cells remain in a multilayer rather than forming a monolayer (Corrales et al., 2006). We therefore analyzed the Purkinje cell layer in the *En1/2* conditional mutants. Based on H&E staining of cerebellar sections, all adult *En1/2* conditional mutants appeared to have a normal monolayer of Purkinje cells (data not shown), suggesting Purkinje cell number is reduced. Analysis of cerebellum sections of control early postnatal mice using CALB1 as a marker for Purkinje cells demonstrated that formation of the Purkinje cell monolayer is nearly complete at P5 (Fig. 7D) (Altman and Bayer, 1997). We therefore examined the Purkinje cell layer at P5 in *En1/2* conditional mutants (n=3 for all *RLd-Cre; VZd-Cre* or *VZd-Cre* or *RLd-Cre* mutants). Except in the most posterior region of *RLd-Cre; VZd-Cre; En1$^{fx/fx}$; En2$^{fx/fx}$* mutants at P5 the CALB1 expressing Purkinje cells had formed a monolayer similar to that of controls (Fig. 7D, H, L & P). These observations suggest that *En1/2* expression in RL-derived cells must indirectly regulate Purkinje cell number prior to P5.

EN1 and EN2 protein transiently persists after deletion of the En1 and En2 alleles

Although we demonstrated using a *R26^{lacZ}* reporter allele that recombination using *VZd-Cre* and *RLd-Cre* begins at e12.5 & e11.5, respectively, and occurs in a majority of VZ-derived and RL-derived cells throughout the medial-lateral axis by e15.5 (Suppl. Figs. 1 & 2), these results do not demonstrate at what time point(s) during development of the cerebellum EN1/2 protein function is lost. Therefore, we analyzed EN1/2 protein expression at three embryonic stages and one postnatal stage in *En1/2* conditional mutants (e13.5, e15.5, e18.5 and P5) (Figs. 9 & 10). During development, *En1/2* expression levels vary along the medial-lateral axis and are observed in the ventricular zone, upper rhombic lip, and a subset of all VZ- and RL-derived cells (Wilson et al., 2011) (Fig. 9A–E and Fig. 10A–D). In *RLd-Cre; VZd-Cre; En1$^{fx/fx}$*; *En2$^{fx/fx}$* conditional mutants, no observable difference in EN1/2 expression was seen in any cells at e13.5 compared to control cerebella (Fig. 9A & F). By e15.5, EN1/2 protein in the vermis was clearly lost in the anterior, but not posterior EGL and little or no decrease was detected in the cerebellar cortex (Fig. 9B–D & G–I). In the hemispheres however, a decrease in EN1/2 expressing cells in the cortex was observed with a similar loss in the anterior EGL (Fig. 9E & J). By e18.5, a significant decrease in EN1/2 protein was observed throughout the cerebellum, except in the posterior EGL (Fig. 10A–C & E–G). By P5, EN1/2 protein was lost from a majority of cells in the cerebellum except the most posterior region of the IGL (posterior lobule IX and lobule X) (Fig. 10D & H).

Comparable results were observed when *En1/2* were removed in VZ- or RL-derived cells (Fig. 9K–T, 10I–P). In *VZd-Cre; En1$^{fx/fx}$*; *En2$^{fx/fx}$* mutants EN1/2 were lost in the cerebellar cortex by e18.5 and as expected, EN1/2 was not decreased in the EGL. Gene ablation in only RL-derived cells (*RLd-Cre; En1$^{fx/fx}$*; *En2$^{fx/fx}$*) resulted in a loss of EN1/2 only in the anterior EGL and expression in the cerebellar cortex appeared normal at all stages. Therefore, loss of EN1/2 protein occurs by e15.5 in anterior RL-derived granule cells in *RLd-Cre* conditional mutants and is lost primarily after e15.5 in VZ-derived cells of the cerebellar cortex in *VZd-Cre* conditional mutants.

DISCUSSION

En2 is required in the progenitor zone cells as well as in their immediate descendents for formation of three fissures and overall cerebellar growth

Our studies uncovered that conditional inactivation of *En2* results in a foliation defect only when *En2* is removed from the VZ and RL by ~e10.5 (*NP-Cre; En2$^{fx/-}$*), but not when it is removed from the VZ- and RL-derived cells (*RLd-Cre; VZd-Cre; En2$^{fx/-}$*). The fissure patterning defects produced using *NP-Cre* are identical to those seen in *En2* null mutants (Joyner et al., 1991; Millen et al., 1994) and extend previous results using ablation of *En2* in all cells of the cerebellum using a *R26^{CreER}* allele (Cheng et al., 2010). Significantly, when *En2* is instead conditionally restored in VZ- and RL-derived cells (*RLd-Cre; VZd-Cre; En2$^{fxlacZ/fxlacZ}$* mutants), the *En2* null mutant cerebellar foliation and growth defects are rescued. Restoration of the *En2* allele in only VZ- or RL-derived cells however, results in only a partial rescue of the fissure patterning defects in the vermis. Although the *En1/2* inactivation and restoration results could appear contradictory, our study of the timing of EN1/2 protein loss in double conditional mutants using the two Cre drivers revealed that conditional inactivation with *VZd-Cre* and *RLd-Cre* does not eliminate EN1/2 protein immediately, but takes several days. EN1/2 proteins are primarily lost in VZ-derived cells between e15.5 and e18.5 and in RL-derived granule cells anterior to lobule IX by e15.5, whereas expression of the *Rosa26$^{lacZ/+}$* allele begins as early as e11.5 or e12.5 with the *RLd-Cre* or *VZd-Cre* alleles, respectively. Thus, it is likely that EN2 protein is not lost early enough using conditional ablation for a foliation and growth phenotype to develop, whereas using conditional restoration, EN2 protein is present early enough to rescue both defects. We therefore conclude that expression of *En2* in cells of the VZ and RL, as well as in their immediate descendents is sufficient for full growth of the cerebellum and correct formation of three fissures altered in *En2* null mutants.

En1 and *En2* act together in the progenitor zones to stimulate expansion of the vermis

Our progenitor zone specific conditional knockout of *En1/2* (*NP-Cre; En1$^{fx/-}$*; *En2$^{fx/-}$* mutants) revealed new requirements for *En1/2* in the VZ and RL. First, we found that *En1/2* expression in the progenitor zones prior to ~e11, is sufficient for specification, but not full expansion of the cerebellum. At e18.5 in *NP-Cre; En1$^{fx/-}$*; *En2$^{fx/-}$* mutants, a small cerebellum is present containing cells from both germinal zones including Purkinje and granule cells. These results extend a previous study in which *En1/2* were eliminated in ~60% of all cerebellar cells after ~e12.5 and adult mutants had only a foliation defect in the vermis (Cheng et al., 2010). Furthermore, by comparing the *NP-Cre* phenotype to that of

ablation of *En1/2* in the descendents of the two progenitor zones we uncovered that *En1* and *En2* are required in the progenitor zones after ~e11 preferentially for expansion of the vermis.

En1 and En2 are independently required in cells derived from each progenitor zone for correct timing of formation of multiple vermal fissures and overall cerebellar growth

Our analysis of mutants lacking *En1/2* in VZ-derived cells (after e15.5) with *VZd-Cre* and/or RL-derived cells (after e13.5) with *RLd-Cre* are the first studies to demonstrate that *En1/2* are required outside the progenitor zones for patterning of fissures in the vermis and overall cerebellar growth. In *RLd-Cre; VZd-Cre; En1*$^{fx/fx}$; *En2*$^{fx/fx}$ mutants, formation of two of the four cardinal fissures is greatly disrupted (primary and secondary) as well as two later forming fissures (precentral and prepyramidal). Interestingly, in the hemispheres all fissures, including the ansoparamedian fissure that is lost in *En2* mutants, form normally when *En1/2* are ablated in VZ- and RL-derived cells. This result demonstrates a requirement in only the cells of the germinal zones, and possibly their immediate descendants, for formation of this fissure. Furthermore, we found that *En1* and *En2* are required in VZ-derived cells alone (*VZd-Cre; En1*$^{fx/fx}$; *En2*$^{fx/fx}$ mutants) for the normal timing of formation (and thus the depth) of four fissures (primary, secondary, precentral, prepyramidal). On the other hand, *En1* and *En2* are required in RL-derived cells (*RLd-Cre; En1*$^{fx/fx}$; *En2*$^{fx/fx}$ mutants) preferentially for cerebellar growth. Furthermore, although the timing of formation of the primary, prepyramidal and secondary fissures are altered in *RLd-Cre; En1*$^{fx/fx}$; *En2*$^{fx/fx}$ mutants, unlike *VZd-Cre; En1*$^{fx/fx}$; *En2*$^{fx/fx}$ mutants (and *En2* null mutants) in which the prepyramidal fissure forms earlier than normal and the secondary fissure is greatly delayed, instead the prepyramidal fissure is greatly delayed and the secondary fissure is only slightly delayed. This result suggests that in RL-derived cells, *En1/2* are primarily required for initiation of the prepyramidal fissure, whereas in VZ-derived cells *En1/2* delay (transiently inhibit) formation of the same fissure. Furthermore, double mutant analysis revealed that the function of *En1/2* in VZ-derived cells is dominant over RL-derived cells. One caveat to consider is that since EN1/2 protein is not ablated in all granule cell precursors posterior to the secondary fissure, expression of EN1/2 in a subset of EGL cells that contribute to the secondary fissure might be sufficient to drive relatively normal fissure formation. Nevertheless, *En1/2* must also function in the granule cell lineage to inhibit (delay) formation of the prepyramidal fissure. In summary, *En1/2* have multiple separate roles in distinct subsets of cells for posterior fissure formation. One role in the VZ- and RL-derived cells is to promote formation of the earliest fissure, the primary fissure. Similarly, *En1/2* function in VZ- and to a lesser extent in RL-derived cells to promote early formation of the secondary fissure and later formation of the precentral fissure. An unanticipated role in VZ-derived cells is to inhibit premature formation of the prepyramidal fissure and in RL-derived cells to promote prepyramidal fissure formation.

En1/2 are required in upper rhombic lip-derived cells to cell non-autonomously regulate cerebellar cell number

We found that conditional inactivation of *En1/2* in only RL-derived cells results in a ~20% decrease in cerebellar size. Furthermore, the cerebella of *RLd-Cre; En1*$^{fx/fx}$; *En2*$^{fx/fx}$ mutants forms a nearly complete monolayer of Purkinje cells by P5 despite this hypoplasia. Thus, the

number of Purkinje cells and likely all cell types must be decreased. Therefore, *En1/2* must function cell non-autonomously in RL-derived cells to maintain Purkinje cell number. Since the RL gives rise to the DCN projection neurons in addition to granule cells, it is possible that *En1/2* are required in one or both of these cell types for normal cerebellar development. Future studies in which *En1/2* are ablated in each cell type will distinguish between these possibilities. Moreover, a decrease in Purkinje cell number at P5 might result in a proportional decrease in the overall levels of SHH signaling and in turn a proportional decrease in proliferation of granule cell precursors. Previous analysis of SHH signaling in *En1/2* conditional mutants generated using a $R26^{CreER}$ allele indeed revealed that the HH target gene *Gli1* is expressed in a similar pattern to control mice in the small mutant cerebellum at P3 (Cheng et al., 2010). We have found a similar result in *RLd-Cre* conditional *En1/2* mutants at early postnatal stages (data not shown). Thus, loss of *En1/2* in RL-derived cells could result in reciprocal signaling defects between granule cell precursors and Purkinje cells by first reducing Purkinje cell number, and thus lowering overall SHH signaling, and in turn reducing granule cell number. In addition, *En1/2* might have a cell autonomous role in granule cell precursors for their proliferation, survival and/or differentiation.

The significance of *En1/2* function and cardinal fissure formation

We have demonstrated that *En1/2* are required in both RL- and VZ-derived cells for controlling the timing of formation of the primary and secondary cardinal fissures. In turn, by changing the timing of fissure formation, the size and shape of the adjacent lobules are altered, and thus the target fields of the corresponding afferent neurons. During development, the primary and secondary fissures are the first fissures to form in the cerebellum, and they define the intervening central lobe (Altman and Bayer, 1997; Larsell, 1952). The subsequent development of the preculminate and prepyramidal fissures in higher order vertebrates allows for the formation of lobules I-III and IV/V as well as VI/VII and VIII (Altman and Bayer, 1997; Larsell, 1952). It has been proposed that each lobule should be considered a functionally distinct entity (Welker, 1990), an idea supported by the distinct Purkinje cell gene expression patterns in groups of lobules and distinct afferent circuitry (Ozol et al., 1999; Sillitoe, 2007). Our studies reveal that in viable *En1/2* conditional mutants with the most severe foliation defects the primary and secondary cardinal fissures fail to form resulting in the absence of lobules IV/V and VIII, which are a major component of the target fields for the spinocerebellar system.

Supplementary Material

Refer to Web version on PubMed Central for supplementary material.

Acknowledgments

The authors would like to thank Antonio V. Galvan and Sirisha Gudavalli for help with tissue sectioning, processing and immunofluorescent analysis. We also would like to thank Dr. Isaac Brownell for critical discussions and Dr. Ryan Willet for maintaining some of the lines of mice. This work was supported by a grant to ALJ from the NIH (MH085726).

Abbreviations

VZ	ventricular zone
RL	rhombic lip
DCN	deep cerebellar nuclei
gcs	granule cells
gcps	granule cell precursors
IGL	internal granule cell layer
EGL	external granule cell layer
pc	preculminate
ppy	prepyramidal
pr	primary
prc	precentral
sec	secondary
po	posterolateral
μm	micrometer

References

Altman, J.; Bayer, SA. Development of the Cerebellar System in Relation to its Evolution, Structure and Functions. CRC Press; New York: 1997.

Ben-Arie N, Bellen HJ, Armstrong DL, McCall AE, Gordadze PR, Guo Q, Matzuk MM, Zoghbi HY. Math1 is essential for genesis of cerebellar granule neurons. Nature. 1997; 390:169–72. [PubMed: 9367153]

Bilovocky NA, Romito-DiGiacomo RR, Murcia CL, Maricich SM, Herrup K. Factors in the genetic background suppress the engrailed-1 cerebellar phenotype. J Neurosci. 2003; 23:5105–12. [PubMed: 12832534]

Blaess S, Corrales JD, Joyner AL. Sonic hedgehog regulates Gli activator and repressor functions with spatial and temporal precision in the mid/hindbrain region. Development. 2006; 133:1799–809. [PubMed: 16571630]

Cheng Y, Sudarov A, Szulc KU, Sgaier SK, Stephen D, Turnbull DH, Joyner AL. The Engrailed homeobox genes determine the different foliation patterns in the vermis and hemispheres of the mammalian cerebellum. Development. 2010; 137:519–29. [PubMed: 20081196]

Corrales JD, Blaess S, Mahoney EM, Joyner AL. The level of sonic hedgehog signaling regulates the complexity of cerebellar foliation. Development. 2006; 133:1811–21. [PubMed: 16571625]

Davis CA, Holmyard DP, Millen KJ, Joyner AL. Examining pattern formation in mouse, chicken and frog embryos with an En-specific antiserum. Development. 1991; 111:287–98. [PubMed: 1680044]

Davis CA, Joyner AL. Expression patterns of the homeo box-containing genes En-1 and En-2 and the proto-oncogene int-1 diverge during mouse development. Genes Dev. 1988; 2:1736–44. [PubMed: 2907320]

Davis CA, Noble-Topham SE, Rossant J, Joyner AL. Expression of the homeo box-containing gene En-2 delineates a specific region of the developing mouse brain. Genes Dev. 1988; 2:361–71. [PubMed: 2454212]

Hanks M, Wurst W, Anson-Cartwright L, Auerbach AB, Joyner AL. Rescue of the En-1 mutant phenotype by replacement of En-1 with En-2. Science. 1995; 269:679–82. [PubMed: 7624797]

Hashimoto M, Mikoshiba K. Mediolateral compartmentalization of the cerebellum is determined on the “birth date” of Purkinje cells. J Neurosci. 2003; 23:11342–51. [PubMed: 14672998]

Hoshino M, Nakamura S, Mori K, Kawauchi T, Terao M, Nishimura YV, Fukuda A, Fuse T, Matsuo N, Sone M, Watanabe M, Bito H, Terashima T, Wright CV, Kawaguchi Y, Nakao K, Nabeshima Y. Ptf1a, a bHLH transcriptional gene, defines GABAergic neuronal fates in cerebellum. Neuron. 2005; 47:201–13. [PubMed: 16039563]

Joyner AL, Herrup K, Auerbach BA, Davis CA, Rossant J. Subtle cerebellar phenotype in mice homozygous for a targeted deletion of the En-2 homeobox. Science. 1991; 251:1239–43. [PubMed: 1672471]

Joyner AL, Kornberg T, Coleman KG, Cox DR, Martin GR. Expression during embryogenesis of a mouse gene with sequence homology to the Drosophila engrailed gene. Cell. 1985; 43:29–37. [PubMed: 2416459]

Joyner AL, Martin GR. En-1 and En-2, two mouse genes with sequence homology to the Drosophila engrailed gene: expression during embryogenesis. Genes Dev. 1987; 1:29–38. [PubMed: 2892757]

Kandel, ER.; Schwartz, JH.; Jessell, TM. Principles of Neural Science. McGraw-Hill; 2000.

Kawaguchi Y, Cooper B, Gannon M, Ray M, MacDonald RJ, Wright CV. The role of the transcriptional regulator Ptf1a in converting intestinal to pancreatic progenitors. Nat Genet. 2002; 32:128–34. [PubMed: 12185368]

Kuemerle B, Zanjani H, Joyner A, Herrup K. Pattern deformities and cell loss in Engrailed-2 mutant mice suggest two separate patterning events during cerebellar development. J Neurosci. 1997; 17:7881–9. [PubMed: 9315908]

Larsell O. The morphogenesis and adult pattern of the lobules and fissures of the cerebellum of the white rat. J Comp Neurol. 1952; 97:281–356. [PubMed: 12999992]

Larsell, O. The Comparative Anatomy and Histology of the Cerebellum from Monotremes through Apes. Univ. Minnesota Press; Minneapolis: 1970.

Llinas RR. The cortex of the cerebellum. Sci Am. 1975; 232:56–71. [PubMed: 1114302]

Machold R, Fishell G. Math1 is expressed in temporally discrete pools of cerebellar rhombic-lip neural progenitors. Neuron. 2005; 48:17–24. [PubMed: 16202705]

Manto M. The cerebellum, cerebellar disorders, and cerebellar research--two centuries of discoveries. Cerebellum. 2008; 7:505–16. [PubMed: 18855093]

Mares V, Lodin Z. The cellular kinetics of the developing mouse cerebellum. II. The function of the external granular layer in the process of gyrification. Brain Res. 1970; 23:343–52. [PubMed: 5478302]

Matei V, Pauley S, Kaing S, Rowitch D, Beisel KW, Morris K, Feng F, Jones K, Lee J, Fritzsch B. Smaller inner ear sensory epithelia in Neurog 1 null mice are related to earlier hair cell cycle exit. Dev Dyn. 2005; 234:633–50. [PubMed: 16145671]

Millen KJ, Hui CC, Joyner AL. A role for En-2 and other murine homologues of Drosophila segment polarity genes in regulating positional information in the developing cerebellum. Development. 1995; 121:3935–45. [PubMed: 8575294]

Millen KJ, Wurst W, Herrup K, Joyner AL. Abnormal embryonic cerebellar development and patterning of postnatal foliation in two mouse Engrailed-2 mutants. Development. 1994; 120:695–706. [PubMed: 7909289]

Ozol K, Hayden JM, Oberdick J, Hawkes R. Transverse zones in the vermis of the mouse cerebellum. J Comp Neurol. 1999; 412:95–111. [PubMed: 10440712]

Schuller U, Zhao Q, Godinho SA, Heine VM, Medema RH, Pellman D, Rowitch DH. Forkhead transcription factor FoxM1 regulates mitotic entry and prevents spindle defects in cerebellar granule neuron precursors. Mol Cell Biol. 2007; 27:8259–70. [PubMed: 17893320]

Sgaier SK, Lao Z, Villanueva MP, Berenshteyn F, Stephen D, Turnbull RK, Joyner AL. Genetic subdivision of the tectum and cerebellum into functionally related regions based on differential sensitivity to engrailed proteins. Development. 2007; 134:2325–35. [PubMed: 17537797]

Sgaier SK, Millet S, Villanueva MP, Berenshteyn F, Song C, Joyner AL. Morphogenetic and cellular movements that shape the mouse cerebellum; insights from genetic fate mapping. Neuron. 2005; 45:27–40. [PubMed: 15629700]

Sillitoe RV, Stephen D, Lao Z, Joyner AL. Engrailed homeobox genes determine the organization of Purkinje cell sagittal stripe gene expression in the adult cerebellum. J Neurosci. 2008; 28:12150–62. [PubMed: 19020009]

Sillitoe RV, Vogel MW, Joyner AL. Engrailed homeobox genes regulate establishment of the cerebellar afferent circuit map. J Neurosci. 2010; 30:10015–24. [PubMed: 20668186]

Soriano P. Generalized lacZ expression with the ROSA26 Cre reporter strain. Nat Genet. 1999; 21:70–1. [PubMed: 9916792]

Sudarov A, Joyner AL. Cerebellum morphogenesis: the foliation pattern is orchestrated by multi-cellular anchoring centers. Neural Dev. 2007; 2:26. [PubMed: 18053187]

Sudarov A, Turnbull RK, Kim EJ, Lebel-Potter M, Guillemot F, Joyner AL. Ascl1 genetics reveals insights into cerebellum local circuit assembly. J Neurosci. 2011; 31:11055–69. [PubMed: 21795554]

Tronche F, Kellendonk C, Kretz O, Gass P, Anlag K, Orban PC, Bock R, Klein R, Schutz G. Disruption of the glucocorticoid receptor gene in the nervous system results in reduced anxiety. Nat Genet. 1999; 23:99–103. [PubMed: 10471508]

Welker WI. The significance of foliation and fissuration of cerebellar cortex. The cerebellar folium as a fundamental unit of sensorimotor integration. Arch Ital Biol. 1990; 128:87–109. [PubMed: 2268185]

Wilson SL, Kalinovsky A, Orvis GD, Joyner AL. Spatially Restricted and Developmentally Dynamic Expression of Engrailed Genes in Multiple Cerebellar Cell Types. Cerebellum. 2011

Wingate RJ, Hatten ME. The role of the rhombic lip in avian cerebellum development. Development. 1999; 126:4395–404. [PubMed: 10498676]

Wurst W, Auerbach AB, Joyner AL. Multiple developmental defects in Engrailed-1 mutant mice: an early mid-hindbrain deletion and patterning defects in forelimbs and sternum. Development. 1994; 120:2065–75. [PubMed: 7925010]

Zervas M, Millet S, Ahn S, Joyner AL. Cell behaviors and genetic lineages of the mesencephalon and rhombomere 1. Neuron. 2004; 43:345–57. [PubMed: 15294143]

Highlights

Ablation of *En1* and *En2* in ventricular zone-derived cells results in significant changes in foliation. Ablation of *En1* and *En2* in upper rhombic lip-derived cells results in a significant reduction of cerebellar growth. *En1* and *En2* regulate the timing of formation of specific fissures differentially in ventricular zone- versus rhombic lip-derived cells. *En2* is required only transiently in ventricular zone cells and their immediate descendents to regulate cerebellar growth and foliation.

- *En2* is required in progenitor zones for formation of fissures and cerebellar growth
- *En1/2* both regulate formation of additional fissures and extensive cerebellar growth
- *En1/2* in ventricular zone-derived cells plays a significant role in fissure formation
- *En1/2* in upper rhombic lip-derived cells are important to regulate cerebellar growth
- *En1/2* act jointly in multiple cerebellar cell types for normal cerebellar development

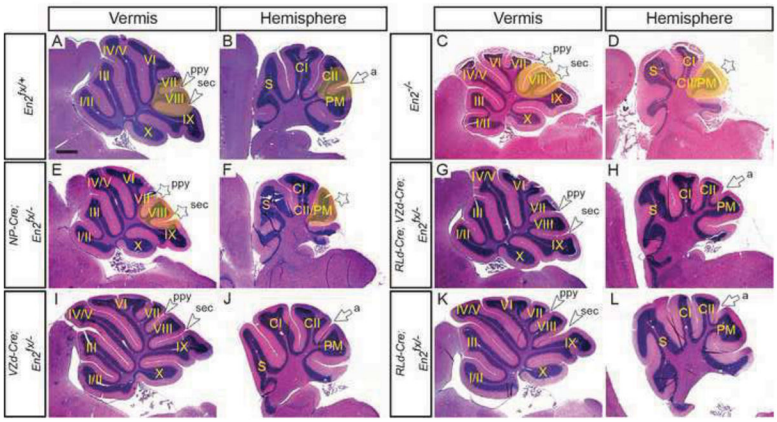

Fig. 1.

Inactivation of *En2* results in a foliation patterning defect only when *En2* is removed early and in cells of the two progenitor zones (VZ and RL). Hematoxylin and Eosin (H&E)-stained sagittal sections of the vermis (A, C, E, G, I & K) and hemispheres (B, D, F, H, J & L) of *En2* conditional mutant with the genotypes indicated. Conditional inactivation in the two progenitor zones (E & F), but not VZ- and RL-derived cells (G–L) results in an $En2^{-/-}$ foliation and size defect. a, ansoparamedian; ppy, prepyramidal; sec, secondary; white arrowheads, vermal posterior fissures; white arrow, hemisphere fissure. Stars denote fissures with developmental defects and yellow highlighted areas denote regions with defects in mutants compared to same region in the control. Scale bar: 600μm.

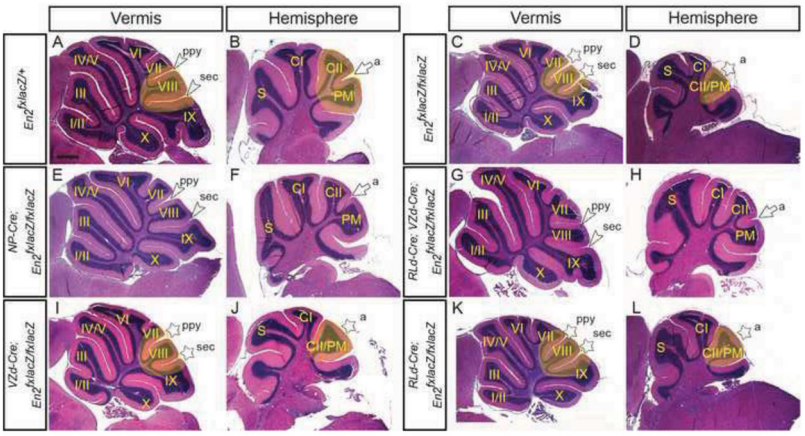

Fig. 2.

Conditional restoration of the *En2* locus in specific cell populations reveals a requirement for *En2* in early descendents of the progenitor zones. H&E-stained sagittal sections of the vermis (A, C, E, G, I & K) and hemispheres (B, D, F, H, J & L) of the genotypes indicated. Conditional restoration of *En2* in VZ and RL (E & F) and VZ/RL-derived cells (G & H), but not VZ-derived or RL-derived cells alone (I–L) rescued the $En2^{-/-}$ null phenotype. a, ansoparamedian; ppy, prepyramidal; sec, secondary; white arrowheads, vermal posterior fissures; white arrow, hemisphere fissure. Stars denote fissures with developmental defects and yellow highlighted areas denote regions with defects in mutants compared to same region in the control. Scale bar: 600μm.

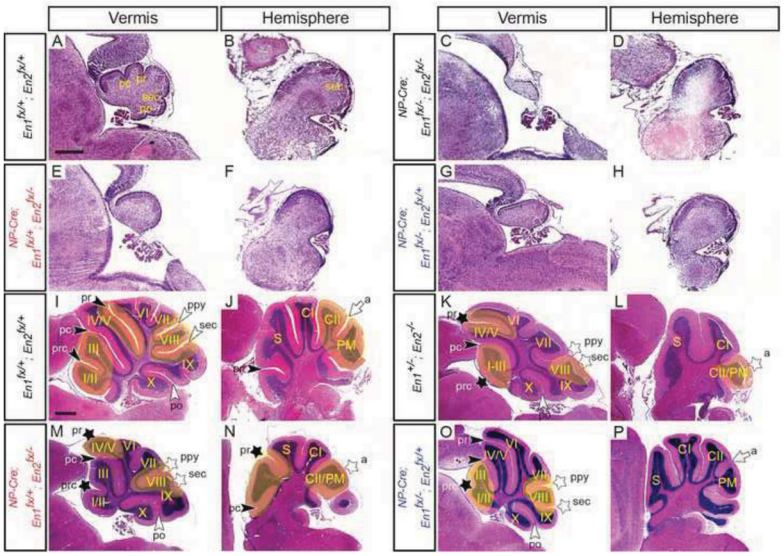

Fig. 3.

Conditional mutations of *En1/2* in the VZ and RL at e10.5 with *NP-Cre* reveals a requirement for *En1/2* in the granule cell lineage for growth of the vermus and foliation defects. Sagittal H&E-stained sections of P0 (A–H) and adult (I–P) mutants with the genotypes indicated showing the vermis (A, C, E, G, I, K, M & O) and hemispheres (B, D, F, H, J, L, N & P). a, ansoparamedian; pc, preculminate; po, posterolateral; prc, precentral; ppy, prepyramidal; pr, primary; sec, secondary; black arrowheads, vermal anterior fissures; white arrowheads, vermal posterior fissures; white arrow, hemisphere fissure. Stars denote fissures with developmental defects and yellow highlighted areas denote regions with defects in mutants compared to same region in the control. Genotypes colored blue represent conditional mutants with one functional allele of *En1* and genotypes colored red represent conditional mutants with one functional allele of *En2*. Scale bar: 400μm for A–H; 600μm for I–P.

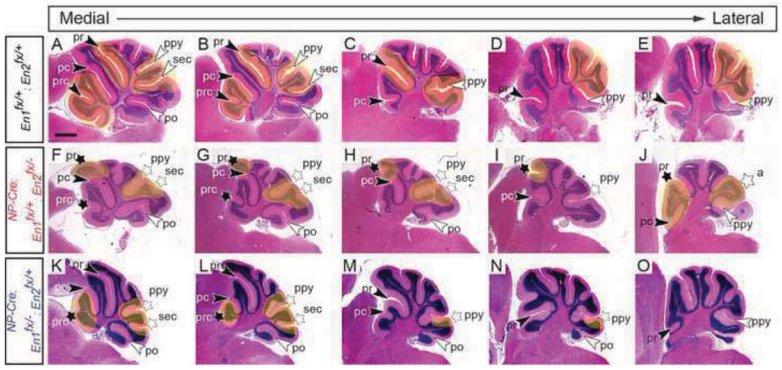

Fig. 4.

Analysis of fissures along the medial to lateral axis in an allelic series of adult *NP-Cre En1/2* conditional mutants reveals a requirement for *En1/2* in neural progenitors and their descendents in formation of multiple fissures. H&E stained sagittal sections from the vermis to hemisphere of mutants with the genotypes indicated. pc, preculminate; po, posterolateral; prc, precentral; ppy, prepyramidal; pr, primary; sec, secondary; black arrowheads, vermal anterior fissures; white arrowheads, vermal posterior fissures. Stars denote fissures with developmental defects and yellow highlighted areas denote regions with defects in mutants compared to same region in the control. Genotypes colored blue represent conditional mutants with one functional allele of *En1* and genotypes colored red represent conditional mutants with one functional allele of *En2*. Scale bar: 600μm.

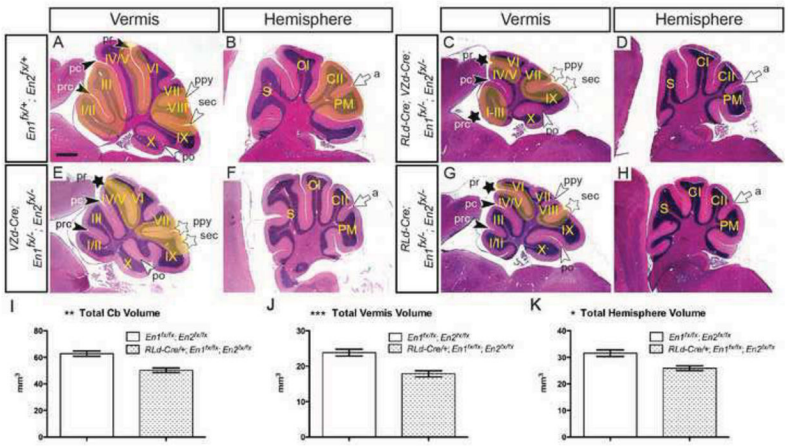

Fig. 5.

Conditional inactivation of *En1* and *En2* in VZ-derived and RL-derived cells using the *VZd-Cre* and *RLd-Cre* alleles reveals independent roles for *En1/2* in each subset of cell types. H&E-stained sagittal sections of the vermis (A, C, E & G) and hemispheres (B, D, F & H) of mice with the genotypes indicated. Volumetric analysis of total cerebellum (I) **p=0.004, vermis (J) ***p=0.001 and hemisphere (K) *p=0.019 in *RLd-Cre; En1*$^{fx/fx}$*; En2*$^{fx/fx}$ adults. a, ansoparamedian; pc, preculminate; po, posterolateral; prc, precentral; ppy, prepyramidal; pr, primary; sec, secondary; black arrowheads, vermal anterior fissures; white arrowheads, vermal posterior fissures; white arrow, hemisphere fissure. Stars denote fissures with developmental defects and yellow highlighted areas denote regions with defects in mutants compared to same region in the control. Scale bar: 600μm.

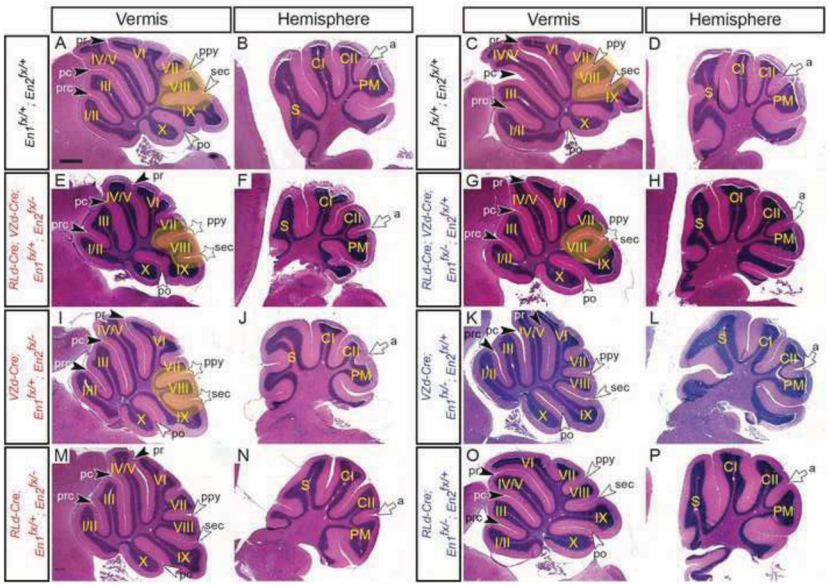

Fig. 6.

Analysis of an allelic series of conditional *En1/2* mutants in VZ-derived and RL-derived cells highlights the predominant role for *En2* in regulating foliation. H&E-stained sagittal sections of the vermis (A, C, E, G, I, K, M & O) and hemispheres (B, D, F, H, J, L, N & P) of mice with the genotypes indicated. a, ansoparamedian; pc, preculminate; po, posterolateral; prc, precentral; ppy, prepyramidal; pr, primary; sec, secondary; black arrowheads, vermal anterior fissures; white arrowheads, vermal posterior fissures; white arrow, hemisphere fissure. Stars denote fissures with developmental defects and yellow highlighted areas denote regions with defects in mutants compared to same region in the control. Genotypes colored blue represent conditional mutants with one functional allele of *En1* and genotypes colored red represent conditional mutants with one functional allele of *En2*. Scale bar: 600μm.

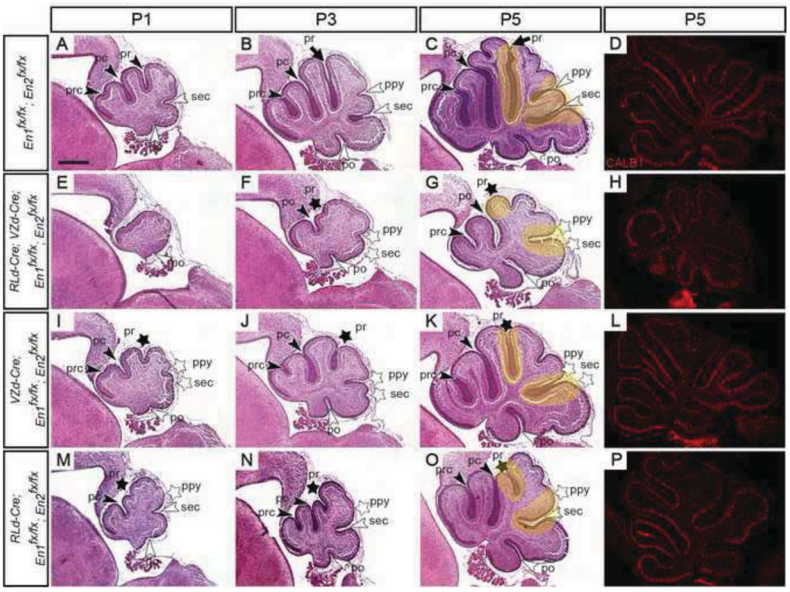

Fig. 7.

Analysis of a postnatal developmental series of VZ- and RL-derived *En1/2* conditional mutants uncovers cell type specific roles in promoting or inhibiting formation of particular fissures. H&E stained sagittal sections of P1 (A, E, I & M), P3 (B, F, J & N) and P5 (C, G, K & O) *En1/2* conditional mutant with the indicated genotypes. In VZ- and RL-derived (E–G), or only VZ-derived (I–K) *En1/2* conditional mutants formation of the primary and secondary fissures is preferentially disrupted. Conditional inactivation of *En1/2* in RL-derived cells (M–O) preferentially disrupts the primary and prepyramidal fissures. Yellow highlighted areas denote regions with defects in mutants compared to same region in the control. Immunostaining for CALB at P5 (D, H, L & P) shows a Purkinje cell monolayer in control and *En1/2* conditional mutants. pc, preculminate; po, posterolateral; prc, precentral; ppy, prepyramidal; pr, primary; sec, secondary; black arrowheads, vermal anterior fissures; white arrowheads, vermal posterior fissures. Stars denote fissures with developmental defects. Scale bar: 400μm.

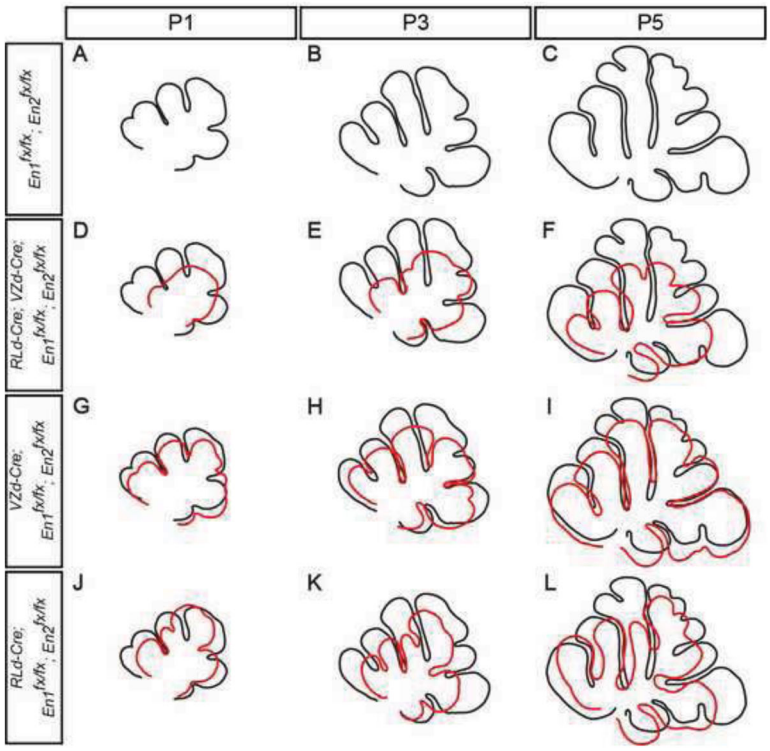

Fig. 8.

Overlay of outlines of sections of cerebella from control (black) and *En1/2* conditional mutants (red) highlights the altered timing of fissure formation in mutants. Outlines of the sections of cerebella shown in Fig. 7 were aligned by matching the bases of fissures with one another.

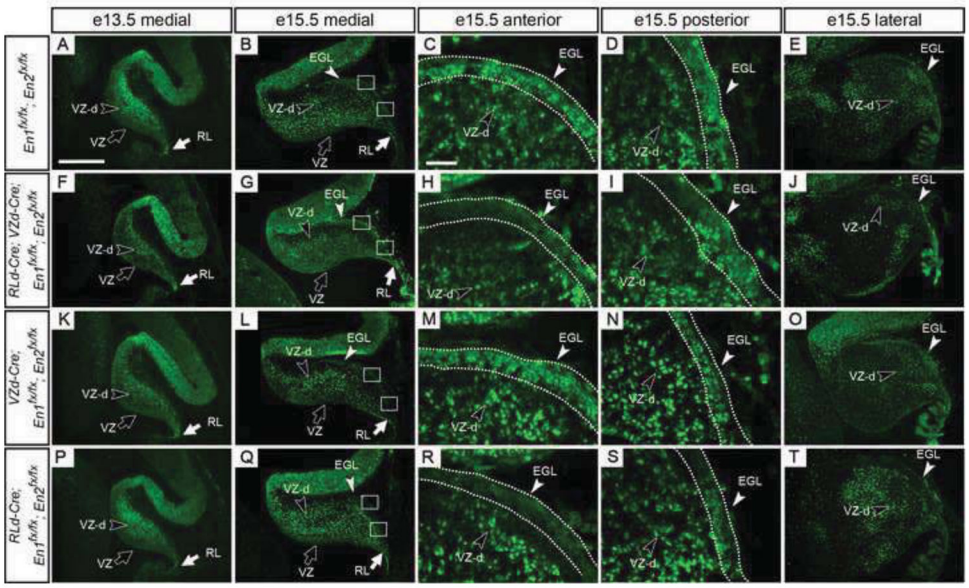

Fig. 9.

Loss of EN1/2 protein is delayed compared to CRE-mediated deletion of the *En* genes. Sagittal sections stained by immunofluorescence for EN1/2 protein in control (A–E) and the *En1/2* conditional mutant embryos indicated (F–T) at e13.5 (A, F, K & P) and e15.5 (B, G, L & Q). High magnification of anterior EGL (C, H, M & R) and posterior EGL (D, I, N & S) and lateral cerebellum (E, J, O & T). At these stages, EN1/2 protein is lost only in cells of the anterior EGL. EGL, external granule layer; RL, upper rhombic lip; RL-d, RL-derived; VZ, ventricular zone; VZ-d; VZ-derived. Scale bar: 300μm for A,B, E,F, I, J, M & N; 50μm for C, D, G, H, K, L O & P.

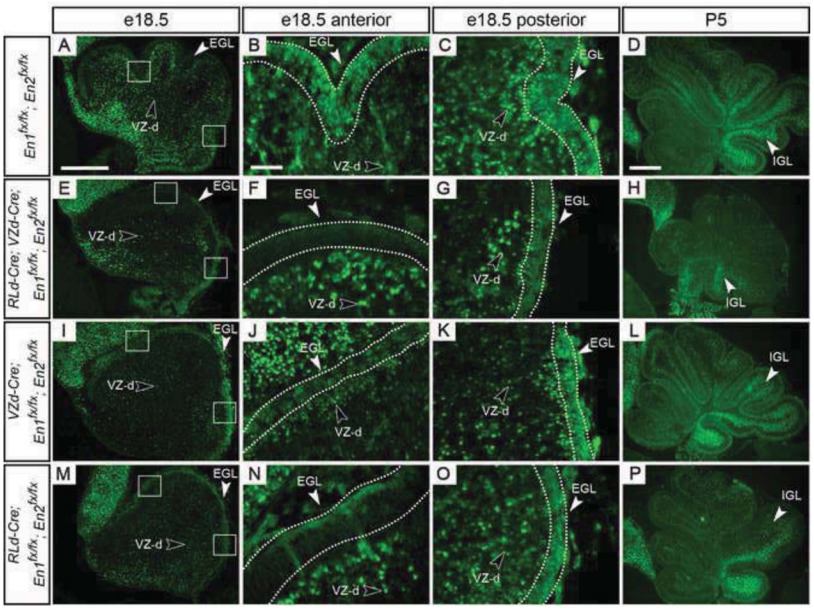

Fig. 10.

EN1/2 protein is greatly reduced in VZ- and RL-derived *En1/2* conditional mutants by e18.5. Sagittal sections stained by immunofluorescence for EN1/2 protein in control (A–D) and mutant (E–P) animals at e18.5 (A–C, E–G, I–K & M–O) and P5 (D, H, L & P). Scale bar: 300μm for A, E, I & M; 50μm for B, C, F, G, J, K, N & O; 400μm for D, H, L & P.

Table 1

Conditional loss of *En1/2* results in foliation defects caused by perturbations in the formation of specific fissures in the vermis and hemispheres. In the vermis, alterations of anterior fissures affect lobules I-V, and disruptions in posterior fissures affect primarily lobule VIII. Anterior fissure defects include an missing or shortened primary (m-pr and s-pr, respectively) and a shortened precentral fissure (s-prc), whereas posterior fissure defects include a deeper prepyramidal (d-ppy) an absent or posteriorly shifted secondary fissure (m-sec and ps-sec, respectively). In the hemispheres, loss of *En1/2* can result in the missing of the ansoparamedian fissure (m-a). Genotypes colored blue represent conditional mutants with one functional allele of *En1* and genotypes colored red represent conditional mutants with one functional allele of *En2*.

	m-pr	s-pr	m-prc	s-prc	m-sec	ps-sec	d-ppy	m-a
NP-Cre; En2$^{fx/-}$	0/4	0/4	0/4	0/4	0/4	4/4	4/4	4/4
RLd-Cre; VZd-Cre; En2$^{fx/-}$	0/4	0/4	0/4	0/4	0/4	0/4	0/4	0/4
VZd-Cre; En2$^{fx/-}$	0/2	0/2	0/2	0/2	0/2	0/2	0/2	0/2
RLd-Cre; En2$^{fx/-}$	0/3	0/3	0/2	0/3	0/3	0/3	0/3	0/3
NP-Cre; En2$^{fxlacZ/fxlacZ}$	0/4	0/4	0/4	0/4	0/4	0/4	0/4	0/4
RLd-Cre; VZd-Cre; En2$^{fxlacZ/fxlacZ}$	0/3	0/3	0/3	0/3	0/3	0/3	0/3	0/3
VZd-Cre; En2$^{fxlacZ/fxlacZ}$	0/4	0/4	0/4	0/4	0/4	4/4	4/4	4/4
RLd-Cre; En2$^{fxlacZ/fxlacZ}$	0/5	0/5	0/5	0/5	0/5	3/5	3/5	5/5
NP-Cre; En1$^{fx/-}$; En2$^{fx/-}$	-	-	-	-	-	-	-	-
NP-Cre; En1$^{fx/+}$; En2$^{fx/-}$	3/3	0/3	0/3	2/3	3/3	0/3	3/3	3/3
NP-Cre; En1$^{fx/-}$; En2$^{fx/+}$	0/4	0/4	3/4	1/4	0/4	4/4	4/4	0/4
RLdCre; VZd-Cre; En1$^{fx/-}$; En2$^{fx/-}$	2/5	3/5	2/5	3/5	5/5	0/5	5/5	0/5
RLd-Cre; VZd-Cre; En1$^{fx/+}$; En2$^{fx/-}$	0/4	0/4	1/4	0/4	0/4	4/4	4/4	0/4
RLd-Cre; VZd-Cre; En1$^{fx/-}$; En2$^{fx/+}$	0/3	0/3	0/3	0/3	0/3	3/3	3/3	0/3
VZd-Cre; En1$^{fx/-}$; En2$^{fx/-}$	0/5	3/5	0/5	1/5	2/5	3/5	5/5	0/5
VZd-Cre; En1$^{fx/+}$; En2$^{fx/-}$	0/3	0/3	0/3	0/3	0/3	2/3	2/3	0/3
VZd-Cre; En1$^{fx/-}$; En2$^{fx/+}$	0/5	0/5	0/3	0/5	0/5	0/5	0/5	0/5
RLd-Cre; En1$^{fx/-}$; En2$^{fx/-}$	0/4	2/4	2/4	0/4	0/4	2/4	0/4	0/4
RLd-Cre; En1^{fx+}; En2$^{fx/-}$	0/3	0/3	0/3	0/3	0/3	1/3	0/3	0/3
RLd-Cre; En1$^{fx/-}$; En2$^{fx/+}$	0/5	0/5	0/5	0/5	0/5	0/5	0/5	0/5
RLd-Cre; VZd-Cre; En1$^{fx/fx}$; En2 $^{fx/fx}$	1/6	5/6	2/6	1/6	6/6	0/6	6/6	0/6

	m-pr	s-pr	m-prc	s-prc	m-sec	ps-sec	d-ppy	m-a
VZd-Cre; En1$^{fx/fx}$*; En2*$^{fx/fx}$	0/8	5/8	1/8	0/8	3/8	5/8	8/8	0/8
RLd-Cre; En1$^{fx/fx}$*; En2*$^{fx/fx}$	0/6	4/6	2/6	0/6	0/6	1/6	0/6	0/6